Time-variations of evapotranspiration rate from Gravity Recovery and Climate Experiment (GRACE) satellite gravimetry

G. Ramillien, Frédéric Frappart, A. Güntner, T. Ngo-Duc, A. Cazenave

Time variations of the regional evapotranspiration rate from Gravity Recovery and Climate Experiment (GRACE) satellite gravimetry

G. Ramillien,[1] F. Frappart,[1,2] A. Güntner,[3] T. Ngo-Duc,[4] A. Cazenave,[1] and K. Laval[4]

Received 9 June 2005; revised 24 April 2006; accepted 12 May 2006; published 4 October 2006.

[1] Since its launch in March 2002, the Gravity Recovery and Climate Experiment (GRACE) mission has been measuring the global time variations of the Earth's gravity field with a current resolution of ~500 km. Especially over the continents, these measurements represent the integrated land water mass, including surface waters (lakes, wetlands and rivers), soil moisture, groundwater, and snow cover. In this study, we use the GRACE land water solutions computed by Ramillien et al. (2005a) through an iterative inversion of monthly geoids from April 2002 to May 2004 to estimate time series of basin-scale regional evapotranspiration rate and associated uncertainties. Evapotranspiration is determined by integrating and solving the water mass balance equation, which relates land water storage (from GRACE), precipitation data (from the Global Precipitation Climatology Centre), runoff (from a global land surface model), and evapotranspiration (the unknown). We further examine the sensibility of the computation when using different model runoff. Evapotranspiration results are compared to outputs of four different global land surface models. The overall satisfactory agreement between GRACE-derived and model-based evapotranspiration prove the ability of GRACE to provide realistic estimates of this parameter.

Citation: Ramillien, G., F. Frappart, A. Güntner, T. Ngo-Duc, A. Cazenave, and K. Laval (2006), Time variations of the regional evapotranspiration rate from Gravity Recovery and Climate Experiment (GRACE) satellite gravimetry, *Water Resour. Res.*, *42*, W10403, doi:10.1029/2005WR004331.

1. Introduction

[2] Temporal change of evapotranspiration (ET) provides precious indications of the global water cycle and climate change, as well as important boundary conditions for climate models. Unfortunately, there are no global-scale in situ measurements of ET. Algorithms for deriving ET from the raw satellite observations require location-specific calibration, making them very difficult to apply globally. In global land surface models (LSMs), ET is modeled through different empirical approaches, e.g., using the Penman equation [*de Marsily*, 1981], through parameterization of the latent heat flux [*Ducoudré et al.*, 1993; *Milly and Shmakin*, 2002] according to the bulk equation introduced by *Monteith* [1963]. At large scales, the temporal distribution of ET is a function of climatic conditions, soil moisture availability, the vegetation type as well as the area of the surface water (wetlands and rivers). These surface conditions are poorly known for global-scale modeling. Existing models provide substantially dissimilar estimates at monthly, seasonal and even annual timescales [*Verant et al.*, 2004].

[3] Recent results of the total land water storage based on the GRACE (Gravity Recovery and Climate Experiment) space mission [*Rodell and Famiglietti*, 1999; *Tapley et al.*, 2004; *Wahr et al.*, 2004; *Schmidt et al.*, 2006; *Ramillien et al.*, 2005a] suggest that the variations of continental water storage are mainly seasonal and the largest amplitudes are located in the large tropical basins of Africa and South America, in the South East Asia during monsoon events, as well as in the high-latitude regions of the Northern hemisphere due to the snow. These patterns are consistent with those provided by global LSMs, such as the water gap global hydrology model (WGHM) [*Döll et al.*, 2003], the land dynamics model (LAD) [*Milly and Shmakin*, 2002], the Global Land Data Assimilation System (GLDAS) [*Rodell et al.*, 2004a] and the organizing carbon and hydrology in dynamics ecosystems model (ORCHIDEE) [*Verant et al.*, 2004]. *Rodell et al.* [2004b] computed time series of ET over the Mississippi River basin, using the land water information from the monthly GRACE geoids combined with precipitation and runoff data. *Rodell et al.* [2004b] showed that the GRACE-derived ET is comparable to the estimates provided by the ECMWF (European Center for Medium range Weather Forecasting) reanalysis and the GLDAS models.

[4] In this paper, we compute time variations of basin-scale ET rates (and associated uncertainties) by time

[1] Laboratoire d'Études en Géophysique et Océanographie Spatiales, UMR 5566, CNRS, CNES, IRD, UPS, Observatoire Midi-Pyrénées, Toulouse, France.
[2] Laboratoire des Mécanismes et Transferts en Géologie, UMR 5572, CNRS, IRD, UPS, Toulouse, France.
[3] GeoForschungZentrum, Telegrafenberg, Potsdam, Germany.
[4] Laboratoire de Météorologie Dynamique, IPSL, Paris, France.

0043-1397/06/2005WR004331

integrating, and then solving, the water mass balance equation, using land water solutions derived from GRACE [*Ramillien et al.*, 2004, 2005a] and independent information on precipitation and runoff. We present estimates of ET, and associated errors, for sixteen drainage basins from April 2002 up to May 2004. For validation, we compare the ET estimates with predictions from global LSMs.

2. Method of Analysis: Water Mass Balance Equation

[5] For a given watershed, the instantaneous equation of the water mass balance is

$$P = \frac{\partial W}{\partial t} + ET + R \tag{1}$$

where P, $\frac{\partial W}{\partial t}$, R are precipitation, water mass storage and runoff respectively. These terms are generally expressed in terms of water mass (mm of equivalent water height) or pressure (kg/m^2) per day. Time integration of equation (1) between times t_1 and t_2 (the starting and the ending dates of the considered period, with $\Delta t = t_2 - t_1$, assumed to be ~30 day, the average time span over which the GRACE geoids are provided) gives

$$\Delta ET = \frac{1}{\Delta t}[\Delta P - \Delta R - \Delta W] \tag{2}$$

In equation (2) above, ET is expressed in mm/day. If we have high-frequency sampled data (e.g., daily data for precipitation), the classical method of the "rectangle" summation has been applied to integrate precipitation P and runoff R over the Δt time interval. ΔW is the variation of the water mass inside the drainage basin area between t_1 and t_2. This term is directly computed as the difference between two monthly GRACE solutions:

$$\Delta W = W(t_2) - W(t_1) \tag{3}$$

The GRACE-based land water solutions computed by *Ramillien et al.* [2005a] are spherical harmonics of a surface density function $F(\theta, \lambda, k)$ that represents the global map of W:

$$F(\theta,\lambda,k) = \sum_{n=1}^{N}\sum_{m=0}^{n}\left[C_{nm}^{F}(k)\cos(m\lambda) + S_{nm}^{F}(k)\sin(m\lambda)\right] \cdot \tilde{P}_{nm}(\cos\theta) \tag{4}$$

In equation (4), θ and λ are colatitude and longitude, k is a given monthly solution. n and m are degree and order, $\tilde{P}_{nm}$ is the associated Legendre function, and $C_{nm}{}^{F}(t)$ and $S_{nm}^{F}(t)$ are the normalized coefficients of the decomposition. In practice, the spherical harmonic development cutoff N used for the land water solutions of *Ramillien et al.* [2005a] is limited to degree 30. This corresponds to a spatial resolution of 660 km.

[6] Instead of using the "time-piecewise" approach proposed earlier by *Rodell et al.* [2004b] that requires high-frequency data (and those were not available) to evaluate equation (3), we linearly approximate the water mass variations of month 'k' as

$$\Delta W_k \approx \frac{1}{2}(\delta W_{k+1} - \delta W_{k-1}) \tag{5}$$

Missing monthly land water solutions data (due to the lack of GRACE geoids) are simply interpolated from the previous and the next months.

[7] Precipitation and runoff data are provided as monthly grids of $1^\circ \times 1^\circ$ (see section 3). Thus to be consistent with the land water solutions, we develop gridded P and R data into spherical harmonics, low-pass filter at degree 30 and recompute gridded data using equation (4).

[8] Sixteen river basins are considered in this study. Their location is shown in Figure 1. The contour of each basin is based on a mask of 0.5° resolution from *Oki and Sud* [1998]. For each month 'k', gridded ΔP, ΔR, and ΔW are spatially averaged over each river basin according to:

$$\overline{F}_k = \frac{R_e^2}{S}\sum_{j\in S} F(\theta_j,\lambda_j,k)\,\delta\lambda\delta\theta\sin\theta_j \tag{6}$$

where F_k represents either ΔP, ΔR or ΔW. $\delta\lambda$ and $\delta\theta$ are grid steps in longitude and latitude respectively (generally $\delta\lambda = \delta\theta$), and R_e is mean Earth's radius (~6378 km).

[9] Once each quantity is averaged spatially, it is easy to compute mean ET using equation (2). Monthly ET values were further divided by a factor of 30 to convert the unit of mm/month into mm/day.

[10] As equation (2) is linear and neglecting interpolation errors in equation (5), one can easily compute associated absolute errors from the relative uncertainties ε_P and ε_R on P and R respectively:

$$\sigma_{ET} \approx \varepsilon_P\Delta P + \varepsilon_R\Delta R + 2\frac{\bar{\sigma}_W}{\Delta t} \tag{7}$$

σ_W is the total error for a single month GRACE solution. Relative uncertainty on precipitation fields ε_P is assumed ~11% [*Rodell et al.*, 2004b]. However, modeled runoff data are much more uncertain, especially in large low-land watersheds such as the Amazon basin. In situ measurements of Amazon discharges vary by 30%: observed annual averages are 155,000 m^3/s [*Vörösmarty et al.*, 1996], and 170,000–200,000 m^3/s [*Dunne et al.*, 1998; *Mertes et al.*, 1996; *Meade et al.*, 1991].

[11] Regional runoff from different models, even for well-constrained regions like in the US, can vary up to a factor of four [*Lohmann et al.*, 2004]. This suggests the situation must be worse elsewhere. Thus we considered ~30% as realistic values for ε_R.

[12] *Wahr et al.* [2004] estimated σ_W to be ~18 mm for 750 km spatial average GRACE-based land water solutions. *Ramillien et al.* [2005b] found $\sigma_W \sim 15$ mm for the final a posteriori uncertainties on the land water solutions, at the spatial resolution of 660 km. As we use a geographical mean to average the land water signal over each basin, $\overline{\sigma}_W <$ 1 mm. Thus, for each monthly estimate, the contribution of the land water to the total budget error (equation (7)) should be no much than 0.07 mm/day.

3. Data Used in This Study

3.1. Land Water Solutions Estimated From GRACE

[13] As explained above, here we use the land water solutions presented by *Ramillien et al.* [2005a]. These solutions range from April 2002 to May 2004, with a few missing months. They consist of total land water mass (surface waters: rivers, lakes, floodplains; soil

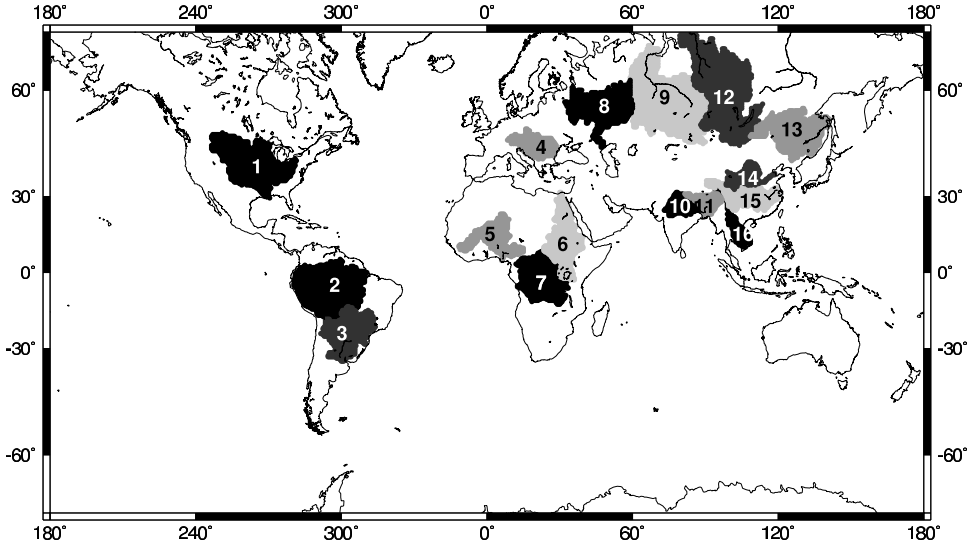

Figure 1. Global distribution of the 16 drainage basins chosen in this study: 1, Mississippi; 2, Amazon; 3, Parana; 4, Danube; 5, Niger; 6, Nile; 7, Congo; 8, Volga; 9, Ob; 10, Ganges; 11, Brahmaputra; 12, Yenisey; 13, Amur; 14, Huang Ho; 15, Yangtse; 16, Mekong.

moisture; groundwater; snow). Their spatial resolution is 660 km. Associated a posteriori uncertainties are also provided.

3.2. Other Data Sets Used in This Study for the Period 2002–2004

3.2.1. Precipitation Data

[14] We use the monthly Global Precipitation Climatology Centre (GPCC) products [*Rudolf et al.*, 1994]. These are gridded data sets based on rain gauge observations, which have been checked using a high-level quality control system [*Rudolf et al.*, 2003]. We used the products with the 1° by 1° geographical latitude and longitude resolution that contain monthly precipitation totals (mm/month) derived from records of 30,000 to 40,000 gauge stations.

3.2.2. Runoff Data

[15] For runoff, we use the predicted values from two LSMs: the WGHM model [*Döll et al.*, 2003] and the LAD model [*Milly and Shmakin*, 2002].

3.2.2.1. Runoff From WGHM

[16] WGHM was specifically designed to estimate river discharge for water resources assessments. It computes 0.5° × 0.5° gridded time series of monthly runoff and river discharge and is tuned against time series of annual rivers discharges measured at 724 globally distributed stations. Surface runoff is computed from the water balance equation that takes into account the water content within the effective root zone, the effective precipitation and the ET. This vertical water balance of the land and open water fraction of each cell is coupled to a lateral transport scheme, which routes the runoff through series of storages within the cell and then transfers the resulting cell outflow to the downstream cell. It is assumed that surface/subsurface runoff is routed to surface storage without delay. Other products of the model are monthly gridded time series of snow depth, soil water within the root zone, groundwater and surface water storage in rivers, lakes and wetlands, ET.

3.2.2.2. Runoff From LAD

[17] The LAD model [*Milly and Shmakin*, 2002] provides monthly 1° × 1° gridded time series of surface parameters. For each cell of the model, the total water storage is composed of three stores: a snowpack store, a root zone store and a groundwater store and the total energy storage is equal to the sum of latent heat of fusion of the snowpack and the glacier and sensible heat content. Runoff generation in the LAD model is essentially a soil-store-excess mechanism, with no limitation on infiltration capacity [*Milly et al.*, 2002], according to the Manabe's simple model [*Manabe*, 1969]. Root zone water does not exceed a specified maximum amount (i.e., the field capacity). This simplified scheme for modeling runoff assumes instantaneous downstream flow of all runoff, so that surface water storage is neglected. Discharge past any point on the river corresponds to the summation over all upstream cells of the product of runoff rate and cell area at that time.

3.3. ET Predictions From Four Different Land Surface Models

[18] GRACE-derived ET is compared to predictions from four global LSMs. We present below how this hydrological parameter is computed by these models.

3.3.1. ET Predictions From WGHM

[19] In WGHM, ET is computed as a function of potential ET (the difference between the maximum potential ET and the canopy transpiration), the soil water content in the effective root zone and the total available soil capacity as

$$ET = \min\left(E_{pot} - E_c, \left(E_{pot\,\max} - E_c\right)\frac{S_s}{S_{s\,\max}}\right) \qquad (8)$$

where E_{pot} is potential ET (mm/day), E_c is evaporation from the canopy (mm/day), $E_{pot\ \max}$ is maximum potential ET (mm/day), S_s is soil water content within the effective root zone (mm), $S_{s\ \max}$ is total available soil water capacity within the effective root zone (mm). These 1° × 1° (originally 0.5° × 0.5°) gridded monthly data are available for 2002 to 2004.

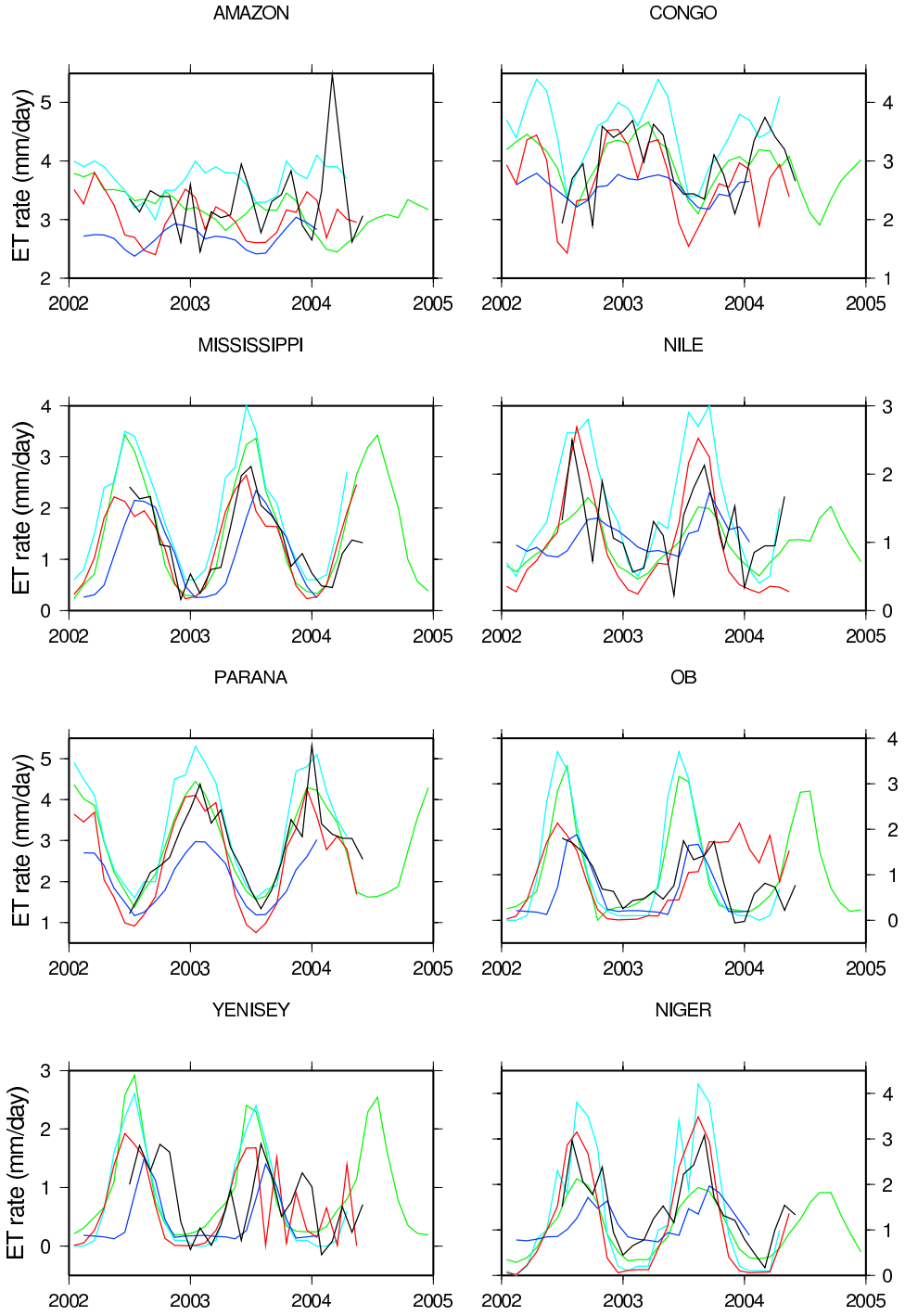

Figure 2. Time series of the ET rate for the 16 drainage basins that were computed from the land waters GRACE solutions [*Ramillien et al.*, 2005a] at the resolution of ~660 km (maximum harmonic degree is 25–30) and combining with precipitation (GPCC) and runoff data (here WGHM) for the same months. Our GRACE-based estimates are plotted in black, ET profiles from WGHM are in red, ORCHIDEE is in dark blue, GLDAS is in green, and LAD is in light blue. Results of the statistical comparison are presented on Table 1.

3.3.2. ET Predictions From LAD

[20] In the LAD model, ET is parameterized as

$$ET = \frac{\rho_a}{r_a + r_s}(q_s(T_0) - q_a)\min\left(\frac{W_R}{0.75W_R^*}, 1\right) \quad (9)$$

where ρ_a is the density of the air, r_a is the aerodynamic resistance for scalar transfer, r_s is a bulk stomatal resistance under conditions of negligible water stress, $q_s(T_0)$ is the mixing ratio of water vapor associated with saturated conditions at the surface temperature, q_a is the mixing ratio at a given level in the atmospheric surface layer, W_R is the

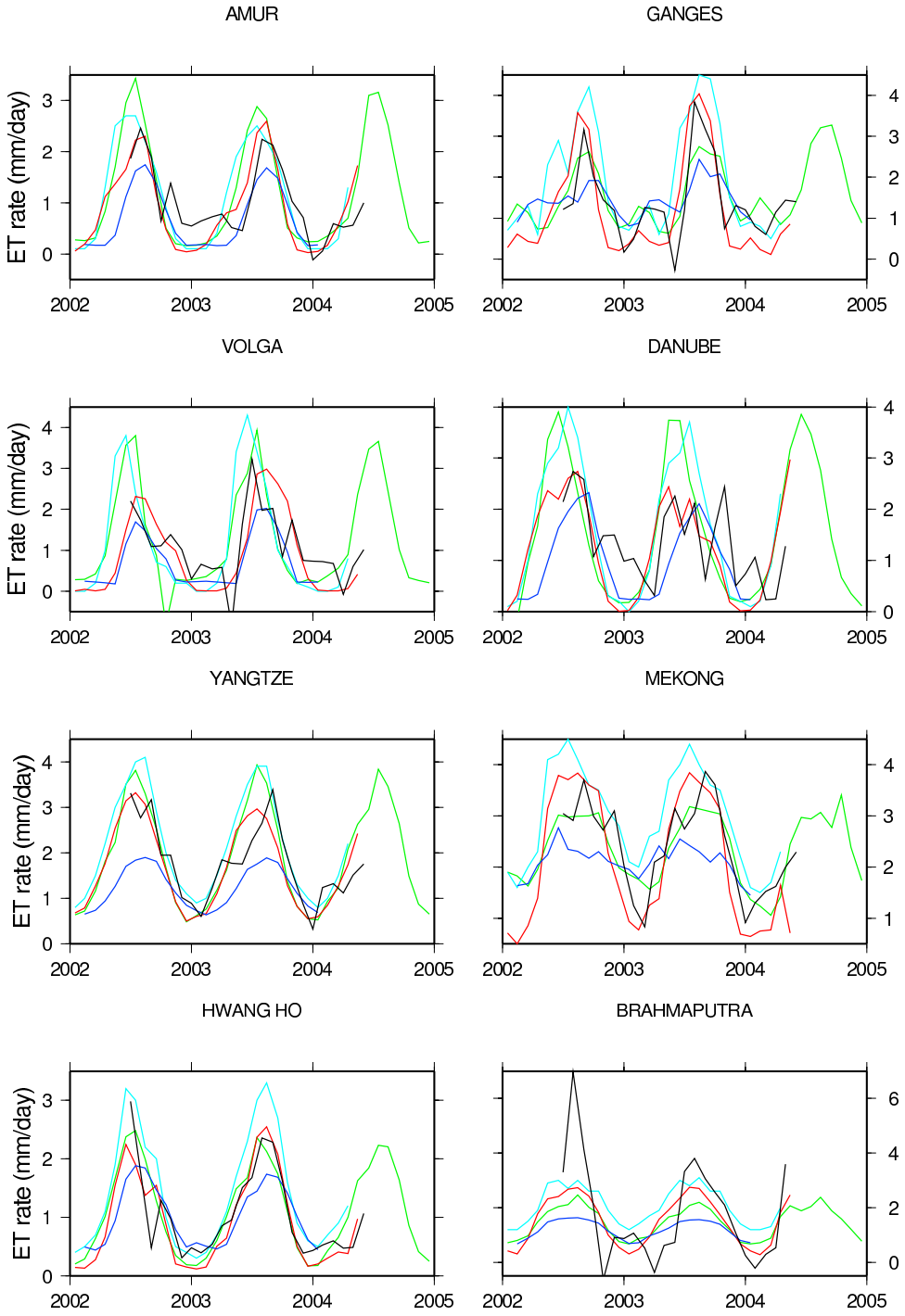

Figure 2. (continued)

water storage in the root zone store, W_R^* is the maximum possible value of W_R. The final factor in equation (9) accounts for the limitation of ET by water stress. The LAD ET outputs are provided from January 1980 to April 2004.

3.3.3. ET Predictions From GLDAS

[21] The GLDAS project is led by scientists of the National Aeronautics and Space Administration (NASA) and the National Oceanic and Atmospheric Administration (NOAA) in association with researchers of the Princeton University, the University of Washington and the Weather Service Office of Hydrology [*Rodell et al.*, 2004a]. Princeton, Washington and OHD participated in North American LDAS project but not GLDAS. This uncoupled land surface assimilation scheme, used for climate studies, is forced by real time outputs of the NCEP (National Centers for Environmental Prediction) reanalysis, satellite data and radar precipitation measurements. Parameters are deduced from high-resolution vegetation, soil coverage and ground elevation data. Data assimilation is performed by one-dimensional Kalman filtering strategy to produce optimal fields of surface parameters. Nominal spatial and temporal resolutions of the grids are 0.25° and 3 hours respectively,

Table 1. Statistical Comparisons Between the Time Series of the GRACE-Based ET Rate (This Study) and the ET Rate Values Provided by Four Global Land Surface Models (GLDAS, LAD, ORCHIDEE, and WGHM) for Each Studied Basin for Bias and RMS Differences and Comparisons for Amazon and Mississippi Basins Using Different Runoff Data as Input (WGHM and LAD)

	GRACE Versus			
Basin	GLDAS	LAD	ORCHIDEE	WGHM
	Bias, mm/d			
Amazon	0.23	−0.31	0.5	0.37
Amur	−0.13	−0.15	0.36	0.09
Brahmaputra	0.32	−0.37	0.7	0.21
Congo	0.02	−0.48	0.33	1.77
Danube	−0.09	−0.26	0.39	0.38
Ganges	−0.11	−0.64	0.1	0.15
Hwang Ho	−0.03	−0.43	0.09	0.06
Mekong	0.08	−0.68	0.43	0.09
Mississippi	−0.16	−0.59	0.25	0.07
Niger	0.39	−0.11	0.36	0.37
Nile	−0.16	−0.59	0.25	0.14
Ob	−0.23	−0.26	0.2	−0.12
Parana	−0.04	−0.46	0.77	0.35
Volga	−0.11	−0.1	0.41	0.02
Yangtze	−0.11	−0.44	0.6	0.07
Yenisey	−0.18	−0.05	0.38	0.04
	RMS, mm/d			
Amazon	0.8	0.65	0.46	0.78
Amur	0.61	0.59	0.4	0.42
Brahmaputra	1.46	1.47	1.65	1.3
Congo	0.5	0.58	0.5	0.55
Danube	0.99	0.97	0.6	0.7
Ganges	0.66	0.97	0.71	0.6
Hwang Ho	0.43	0.5	0.42	0.36
Mekong	0.53	0.49	0.75	0.6
Mississippi	0.48	0.49	0.29	0.32
Niger	0.45	0.95	0.55	1.34
Nile	0.48	0.49	0.29	0.64
Ob	0.75	0.94	0.34	0.82
Parana	0.46	0.66	0.53	0.47
Volga	0.99	0.9	0.55	0.85
Yangtze	0.53	0.51	0.53	0.41
Yenisey	0.75	0.73	0.5	0.75
	GRACE Versus			
Runoff	GLDAS	LAD	ORCHIDEE	WGHM
	RMS, mm/d			
WGHM(Mississippi)	0.48	0.49	0.29	0.32
LAD (Mississippi)	0.53	0.53	0.33	0.35
WGHM (Amazon)	0.8	0.65	0.46	0.6
LAD (Amazon)	0.91	0.64	0.6	0.77

and all fields are defined for all lands north of 60°S. Outputs used in this study were from a 1° resolution simulation of Noah land surface model (GLDAS/Noah) in which data assimilation was not applied. Monthly 1° × 1° means of the ET rates (units: kg/m^2) were interpolated from these nominal 3 hour outputs. Because of problems of simulation in the ET subroutine of GLDAS, the ET rate fields after October 2002 were computed as the ratio of the predicted latent heat flux and the constant latent heat of evaporation (around 2.501 × f 10^6 J/kg) (M. Rodell, personal communication, 2005).

3.3.4. ET Predictions From ORCHIDEE

[22] The ORCHIDEE land surface model [*Verant et al.*, 2004; *Krinner et al.*, 2005], developed at the Institut Pierre Simon Laplace (Paris, France), provides monthly 1° × 1° gridded time series of surface parameters estimated from 1948 to 2003. For this study, we only use the ET output of SECHIBA (Schématisation des Echanges Hydriques l'Interface entre la Biosphère et l'Atmosphère) [*Ducoudré et al.*, 1993; *De Rosnay and Polcher*, 1998], which is the water and energy cycle component of ORCHIDEE. In SECHIBA, the ET flux is described using the bulk equation introduced by *Monteith* [1963], similar to equation (9).

4. Results

[23] Figure 2 presents GRACE-based ET time series for each of the 16 selected river basins. The ET estimates presented in Figure 2 use the WGHM runoff for the computations. For comparison, are also plotted model-based ET (from WGHM, GLDAS, LAD and ORCHIDEE). In view of the short time span considered here, the signal is dominated by the seasonal signal. Maximum of the ET seasonal cycle occur in July for Northern hemisphere river basins and in January in the Southern hemisphere. These are in the range 3–4 mm/day for all basins (at the spatial resolution of ∼660 km). These GRACE-based ET seasonal variations are consistent with model predictions as well as observations. In the central Amazon basin for example, a 3.6 mm/day seasonal amplitude was found by *Costa and Foley* [1999].

[24] Table 1 presents the results of statistical comparisons between GRACE-derived and model-based ET. The RMS (root-mean-square) differences are averaged over the overlapping months over the 2002–2004 period. In general, RMS differences between GRACE-based and model-based ET are less than 1 mm/day, except for the Brahmaputra watershed, a relatively small basin, where RMS differences range from 1.46 to 1.65 mm/day. The lowest RMS difference is found with the ORCHIDEE model over the Mississippi basin (∼0.29 mm/day rms). This result for the Mississippi basin is comparable with that from *Rodell et al.* [2004b]. These authors derived a time series of the ET rate changes by low-pass filtering the GRACE geoids according to the *Wahr et al.* [1998] method. They also found a good agreement with the GLDAS model for monthly means (∼0.83 mm/day rms) (spatial resolution of 750 km). As this basin is well covered by field observations, this comparison confirms the great value of GRACE for estimation ET.

[25] In order to test the impact of the R model values to compute ET (and associated uncertainties), we consider two different river basin cases: the Amazon basin which suffers from lack of observations (we then assume the model error is large in this region), and the Mississippi basin which is well covered by in situ data (thus error on R should be small).

[26] We present GRACE-based ET values using monthly runoff data from two different models (WGHM and LAD) in Figures 3a and 3b. As seen on Figures 3a and 3b, considering LAD runoff produces higher ET than using WGHM runoff: the mean difference between WGHM and LAD curves is a constant bias over the considered time span (1.5 mm/day and 0.40 mm/day for Amazon and Mississippi basins respectively). Besides, the ET rate obtained by using WGHM runoff remains the closest to the mean value proposed by *Costa and Foley* [1999] for the Amazon River basin.

[27] Figures 4a and 4b present ET uncertainties (equation (7)) for the two basins (Amazon and Mississippi). As

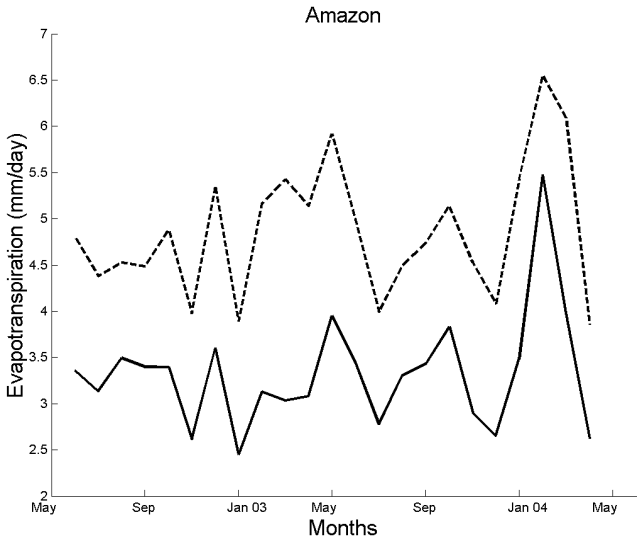

Figure 3a. Time series of the variations of the ET rate over the Amazon basin considering runoff data from different global models: solid line: using R from WGHM model; dashes line: using R from LAD model.

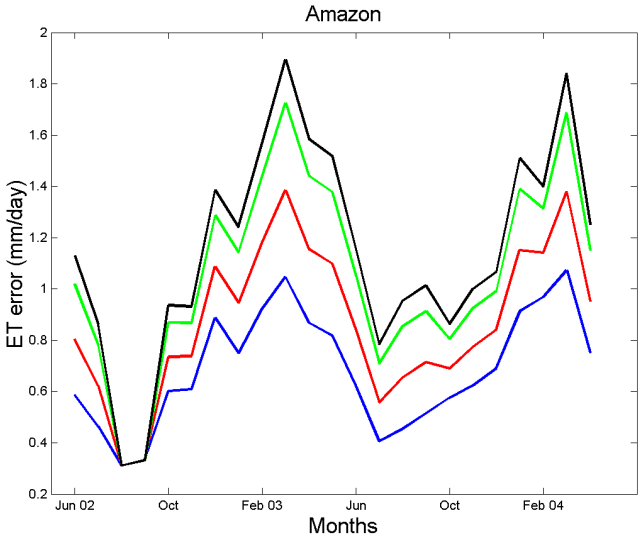

Figure 4a. Time variations of the regional uncertainties on ET estimates over the basin of the Amazon River for different relative errors on the runoff data: ε_R = 5% (blue), 15% (red), 25% (green), and 30% (black).

expected by the accuracy of the model runoff in these two regions, extreme errors (1.8 mm/day, ~50% relative error) are found in the Amazon basin. In the case of the Mississippi basin, the maximum error reaches ~0.55 mm/day (around June 2003) that corresponds to 20% of the amplitude of ET rate. Accuracy of the ET rate estimates should be clearly improved when the quality of the input runoff data from models increases.

5. Summary

[28] In this study, we have developed an approach based on the resolution of the water mass balance equation to derive regional time variations of the ET rate based on GRACE data. We also estimate absolute errors associated with the GRACE-based ET time series, from the relative uncertainties on precipitation and runoff. These absolute errors reach up to 1/6 of the seasonal amplitudes of the estimated ET. Comparison of the GRACE-based ET with different global LSMs ET estimates shows good overall agreement, especially at the seasonal timescale.

[29] In the future, new GRACE land water solutions would be considered as input to the proposed approach to complete the series of ET rate variations. ET rate estimation by combining both space gravimetry data and model outputs would provide further information on processes at the Earth's surface, such as vegetation distribution and soil type.

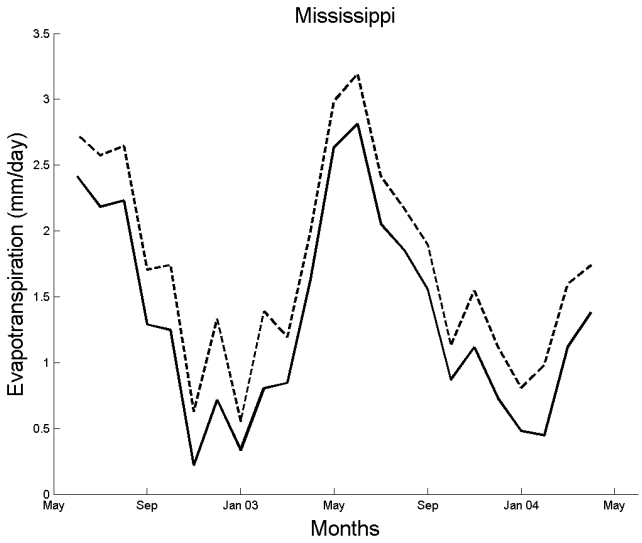

Figure 3b. Same as Figure 3a but for the Mississippi basin.

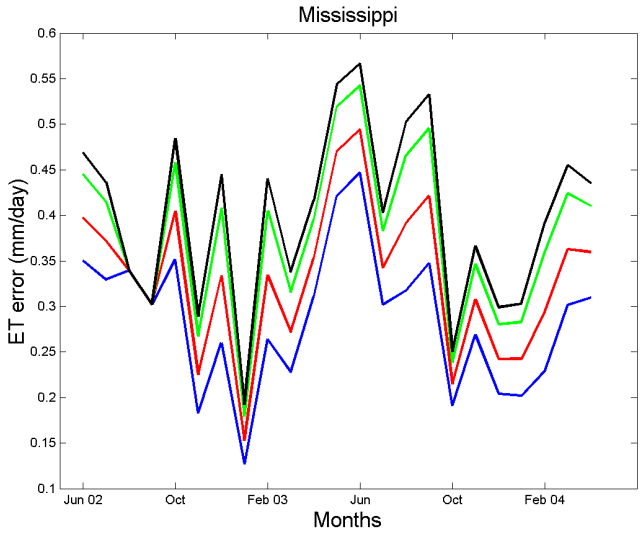

Figure 4b. Same as Figure 4a but for the Mississippi basin.

[30] **Acknowledgments.** We would like to thank Petra Döll, Chris Milly, and Matthew Rodell for having made the monthly outputs of their models available to us. This work was partly funded by the French Programme National de Télédection Spatiale (PNTS). One of us (F.F.) benefited from a CNES-ALCATEL SPACE Ph.D. grant.

References

Costa, M. H., and J. A. Foley (1999), Trends in the hydrologic cycle of the Amazon basin, *J. Geophys. Res.*, *104*, 14,189–14,198.

de Marsily, G. (1981), *Hydrologie Quantitative*, 217 pp., Masson, Paris.

De Rosnay, P., and J. Polcher (1998), Modeling root water uptake in a complex land surface scheme coupled to a GCM, *Hydrol. Earth Syst. Sci.*, *2*(2–3), 239–256.

Döll, P., F. Kaspar, and B. Lehner (2003), A global hydrological model for deriving water availability indicators: Model tuning and validation, *J. Hydrol.*, *270*, 105–134.

Ducoudré, N., K. Laval, and A. Perrier (1993), SECHIBA: A new set of parametrization of the hydrologic exchanges at the land/atmosphere interface within the LMD atmosphere general circulation model, *J. Clim.*, *6*(2), 248–273.

Dunne, T., L. A. K. Mertes, R. H. Meade, J. E. Richey, and B. R. Forsberg (1998), Exchanges of sediment between the flood plain and channel of Amazon River in Brazil, *Geol. Soc. Am. Bull.*, *110*, 450–467.

Krinner, G., N. Viovy, N. De-Noblet-Ducoudré, J. Ogée, J. Polcher, P. Friedlingstein, P. Ciais, S. Sitch, and C. Prentice (2005), A dynamic global vegetation model for studies of the coupled atmosphere-biosphere system, *Global Biogeochem. Cycles*, *19*, GB1015, doi:10.1029/2003GB002199.

Lohmann, D., et al. (2004), Streamflow and water balance intercomparisons of four land surface models in the North American Land Data Assimilation System project, *J. Geophys. Res.*, *109*, D07S91, doi:10.1029/2003JD003517.

Manabe, S. (1969), Climate and ocean circulation: 1. The atmospheric circulation and the hydrology of the Earth's surface, *Mon. Weather Rev.*, *97*, 739–774.

Meade, R. H., J. M. Rayol, S. C. Da Conceicao, and J. R. G. Natividade (1991), Backwater effects in the Amazon River basin of Brazil, *Environ. Geol.*, *18*, 105–114.

Mertes, L. A. K., T. Dunne, and L. A. Martinelli (1996), Channel-floodplain geomorphology along the Solimões-Amazon River, Brazil, *Geol. Soc. Am. Bull.*, *108*, 1089–1107.

Milly, P. C. D., and A. B. Shmakin (2002), Global modelling of land water and energy balances: 1. The land dynamics (LAD) model, *J. Hydrometeorol.*, *3*, 283–299.

Monteith, J. L. (1963), Gas exchange in plant communities, in *Environmental Control of Plant Growth*, edited by L. T. Evans, pp. 95–112, Springer, New York.

Oki, T., and Y. C. Sud (1998), Design of total runoff integrating pathways (TRIP)—A global river channel network, *Earth Inter.*, *2*, Paper 1, 37 pp.

Ramillien, G., A. Cazenave, and O. Brunau (2004), Global time variations of hydrological signals from GRACE satellite gravimetry, *Geophys. J. Int.*, *158*, 813–826.

Ramillien, G., F. Frappart, A. Cazenave, and A. Güntner (2005a), Time variations of the land water storage from an inversion of 2 years of GRACE geoids, *Earth Planet. Sci. Lett.*, *235*, 283–301.

Ramillien, G., A. Cazenave, C. Reigber, R. Schmidt, and P. Schwintzer (2005b), Recovery of global time variations of surface water mass by GRACE geoid inversion, in *Gravity, Geoid and Space Missions*, *Int. Assoc. Geod. Symp. Ser.*, vol. 129, pp. 310–315, Springer, New York.

Rodell, M., and J. S. Famiglietti (1999), Detectability of variations in continental water storage from satellite observations of the time dependent gravity field, *Water Resour. Res.*, *35*, 2705–2723.

Rodell, M., et al. (2004a), The Global Land Data Assimilation System, *Bull. Am. Meteorol. Soc.*, *85*, 381–394.

Rodell, M., J. S. Famiglietti, J. Chen, S. I. Seneviratne, P. Viterbo, S. Holl, and C. R. Wilson (2004b), Basin scale estimate of evapotranspiration using GRACE and other observations, *Geophys. Res. Lett.*, *31*, L20504, doi:10.1029/2004GL020873.

Rudolf, B., H. Hauschild, W. Rueth, and U. Schneider (1994), Terrestrial precipitation analysis: Operational method and required density of point measurements, in *Global Precipitations and Climate Change*, *NATO ASI Ser., Ser. I*, vol. 26, edited by M. Desbois and F. Desalmond, pp. 173–186, Springer, New York.

Rudolf, B., T. Fuchs, U. Schneider, and A. Meyer-Christoffer (2003), Introduction of the Global Precipitation Climatology Centre (GPCC), report, 16 pp., Dtsch. Wetterdienst, Offenbach, Germany.

Schmidt, R., et al. (2006), GRACE observations of changes in continental water storage, *Global Planet. Change*, *50*, 112–126, doi:10.1016/j.gloplacha.2004.11.018.

Tapley, B. D., S. Bettadpur, M. Watkins, and C. Reigber (2004), The Gravity Recovery and Climate Experiment: Mission overview and early results, *Geophys. Res. Lett.*, *31*, L09607, doi:10.1029/2004GL019920.

Verant, S., K. Laval, J. Polcher, and M. Castro (2004), Sensitivity of the continental hydrological cycle to spatial resolution over the Iberian Peninsula, *J. Hydrometeol.*, *5*(2), 267–285.

Vörösmarty, C. J., C. J. Willmott, B. J. Choudhury, A. L. Schloss, T. K. Stearns, S. M. Robeson, and T. J. Dorman (1996), Analyzing the discharge regime of a large tropical river through remote sensing, ground-based climatic data, and modelling, *Water Resour. Res.*, *32*, 3137–3150.

Wahr, J., M. Molenaar, and F. Bryan (1998), Time-variability of the Earth's gravity field: Hydrological and oceanic effects and their possible detection using GRACE, *J. Geophys. Res.*, *103*, 30,205–30,230.

Wahr, J., S. Swenson, V. Zlotnicki, and I. Velicogna (2004), Time-variable gravity from GRACE: First results, *Geophys. Res. Lett.*, *31*, L11501, doi:10.1029/2004GL019779.

F. Frappart, A. Cazenave, and G. Ramillien, LEGOS, UMR 5566, CNRS, CNES, IRD, UPS, Observatoire Midi-Pyrénées, 18, avenue Edouard Belin, F-31400, Toulouse, France. (ramillie@notos.cst.cnes.fr)

A. Güntner, GeoForschungZentrum, Telegrafenberg, D-14473 Potsdam, Germany.

K. Laval, and T. Ngo-Duc, LMD, IPSL, 4, place Jussieu, F-75252 Paris Cedex 05, France.